

1-Metallacyclopropene Complexes and η^1 -Vinyl Complexes Containing the $\text{Cp}^*\text{W}(\text{NO})$ Fragment

Peter Legzdins,* Sean A. Lumb, and Steven J. Rettig†

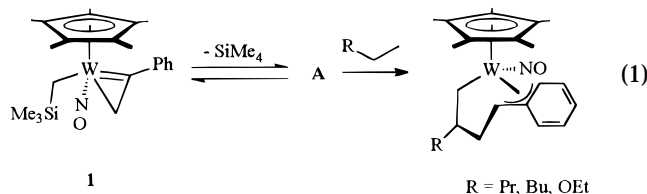
Department of Chemistry, The University of British Columbia,
Vancouver, British Columbia, Canada V6T 1Z1

Received March 12, 1999

The solid-state molecular structure of $\text{Cp}^*\text{W}(\text{NO})(\text{CH}_2\text{SiMe}_3)(\eta^2\text{-CPhCH}_2)$ reveals that the vinyl ligand in this complex exists in a distorted form in the solid state that cannot be readily described by either of the classic η^1 -vinyl or 1-metallacyclopropene limiting structures, by comparison to other crystallographically characterized vinyl complexes reported in the literature. However, the NMR parameters for the CPhCH_2 fragment in this complex are characteristic of those of a 1-metallacyclopropene unit. In addition to these studies, a series of vinyl-containing species of the general formulas $\text{Cp}^*\text{W}(\text{NO})(\eta^2\text{-CPhCH}_2)(\text{X})$ and $\text{Cp}^*\text{W}(\text{NO})(\eta^1\text{-CPh=CH}_2)(\text{LX})$ ($\text{X} = \text{Cl, OTf}$; $\text{LX} = \text{O}_2\text{CPh, NH}^t\text{Bu, (PPh}_3\text{)(H)}$) has been prepared, and the solid-state metrical parameters and solution NMR spectroscopic properties of these complexes have been examined and compared to those of other vinyl-containing complexes reported in the literature. It has been found that the nature of the tungsten–vinyl interaction in these compounds is dependent upon the donor strength of the one-electron (1e) X or 3e LX donor ligands that are also present in the tungsten coordination sphere.

Introduction

We recently reported a unique C–H bond-activation process effected during the thermal activation of an tungsten nitrosyl vinyl complex.¹ Specifically, the dual C–H bond activation of either *n*-pentane or *n*-hexane during the thermal decomposition of $\text{Cp}^*\text{W}(\text{NO})(\text{CH}_2\text{-SiMe}_3)(\eta^2\text{-CPhCH}_2)$ (**1**) to $\text{Cp}^*\text{W}(\text{NO})(\eta^2\text{-PhC}\equiv\text{CH})$ (**A**) in the appropriate hydrocarbon solvent yields the novel tungstenacycles $\text{Cp}^*\text{W}(\text{NO})(\eta^3\text{-CHPh})\text{CH}_2\text{CHRCH}_2$ ($\text{R} = {}^n\text{Pr, } {}^n\text{Bu}$) (eq 1).¹



The preliminary communication of this work described the solid-state molecular structure of **1** as determined by X-ray diffraction methods at ambient temperature.¹ The vinyl-H atoms were not located in the difference map, and the structure showed large anisotropic displacement parameters representing unresolved disorder, most notably in the atoms of the Cp^* ligand. The result was therefore a structure of relatively low precision, affording a somewhat blurred image of the molecule. Definite conclusions regarding the nature of the W–vinyl interaction were difficult to make at that time. Since then, the molecular structure of **1** has been redetermined at 180 K by single-crystal X-ray diffraction

methods. The solid-state characteristics of the CPhCH_2 ligand in **1** have been investigated in greater detail, and the results indicate that, while the $\text{W}-(\text{CPhCH}_2)$ bonding interaction in this complex involves both carbon nuclei of the vinyl moiety, the nature of the interaction is not readily described by a limiting 1-metallacyclopropene bonding mode. The distorted nature of the $\text{W}-(\eta^2\text{-CPhCH}_2)$ interaction in **1** has prompted us to undertake a more detailed investigation of the structural parameters of this fragment. With this goal in mind, a series of vinyl-containing species of the general formulas $\text{Cp}^*\text{W}(\text{NO})(\eta^2\text{-CPhCH}_2)(\text{X})$ and $\text{Cp}^*\text{W}(\text{NO})(\eta^1\text{-CPhCH}_2)(\text{LX})$ ($\text{X} = \text{Cl, OTf}$; $\text{LX} = \text{O}_2\text{CPh, NH}^t\text{Bu, (PPh}_3\text{)(H)}$) has been prepared, on the basis of the presumption that the vinyl fragment will be manifested in either the η^1 or η^2 form under the influence of other one-electron (1e) X or 3e LX donor ligands present in the tungsten coordination sphere. The solid-state metrical parameters and solution NMR spectroscopic properties of these complexes have been examined and compared to those of other η^1 -vinyl and 1-metallacyclopropene complexes reported in the literature and help to shed light on the W–vinyl interaction extant in **1**. The results of these investigations are presented in this paper.

Results and Discussion

A. The Vinyl–Tungsten Interaction in $\text{Cp}^*\text{W}(\text{NO})(\eta^2\text{-CPhCH}_2)(\text{CH}_2\text{SiMe}_3)$ (1**).** The results of the redetermination of the solid-state molecular structure of **1** at 180 K are depicted in Figure 1. In contrast to the findings of our earlier report, the vinyl H atoms (H(16) and H(17)) were located during the refinement of the structural data. In considering the W–vinyl structural parameters, we note that some important features that aid in the identification of an η^1 -vinyl or

* To whom correspondence should be addressed.

† Deceased October 27, 1998.

(1) Debad, J. D.; Legzdins, P.; Lumb, S. A.; Batchelor, R. J.; Einstein, F. W. B. *J. Am. Chem. Soc.* **1995**, *117*, 3288.

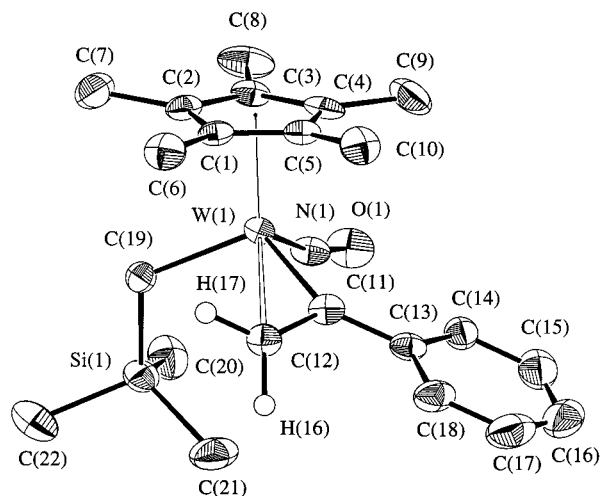


Figure 1. Solid-state molecular structure of **1** with 50% probability thermal ellipsoids depicted. Selected interatomic distances (Å) and angles (deg): W(1)–N(1) = 1.760(3), W(1)–Cp*(centroid) = 2.04, N(1)–O(1) = 1.237(4), W(1)–C(19) = 2.173(5), W(1)–C(11) = 2.076(5), C(11)–C(12) = 1.342(6), C(11)–C(13) = 1.470(7), W(1)–C(12) = 2.615(5), C(12)–H(17) = 1.08(4), C(12)–H(16) = 1.16(5); W(1)–C(11)–C(12) = 97.5(4), N(1)–W(1)–C(19) = 96.0(2), C(12)–C(11)–C(13) = 123.0(4), N(1)–W(1)–C(11) = 96.8(2), C(12)–W(1)–C(19) = 89.8(2), C(11)–W(1)–C(19) = 114.9(2), W(1)–C(11)–C(13) = 137.1(3), H(17)–C(12)–H(16) = 108.9(31), H(17)–C(12)–C(12) = 128.1(20), H(16)–C(12)–C(12) = 122.9(25), C(11)–W(1)–Cp*(centroid) = 113.3, W(1)–C(6)–Si = 117.7(4), W(1)–N(1)–O(1) = 168.6(5).

1-metallacyclopropene unit in the $M(C^1(R)C^2R_2)$ fragment (as depicted below) are the $M-C^1$ and $M-C^2$ bond distances, the $M-C^1-C^2$ bond angle, the $M-C^1-R$ angle, and the C^1-C^2 bond distance.

In the η^1 -vinyl fragment ($M(\eta^1-C^1R=C^2R_2)$), the $M-C^1$ bond distance is typically that of a single $M-C$ bond, the $M-C^2$ distance is greater than the sum of the van der Waals radii of M and C^2 (i.e. the two nuclei are nonbonding), the $M-C^1-C^2$ and $M-C^1-R$ angles are characteristically those of sp^2 -hybridized centers (ca. 120°), and the C^1-C^2 distance is typically that of a $C=C$ bond (ca. 1.34 Å). In contrast, the $M-C^1$ and $M-C^2$ contacts in the 1-metallacyclopropene fragment ($M(\eta^2-C^1R^2C^2R_2)$) are typically those of an $M=C$ bond and an $M-C$ bond, respectively. The $M-C^1-C^2$ angle is contracted ($<90^\circ$) due to the $M-C^2$ bonding interaction, and the $M-C^1-R$ angle is typically expanded beyond 120° in response to the distortion in the $M-C^1-C^2$ angle. The C^1-C^2 distance is typically found to be intermediate between a single and double $C-C$ bond, ca. 1.45 Å.



1-metallacyclopropene

η^1 -vinyl

The W–C(11) bond distance of $2.076(5)$ Å in the molecular structure of **1** borders on those typically found for 1-metallacyclopropene $M=C$ linkages (vide supra: $M = Mo, W, Re$; $1.9–2.0$ Å)² and is comparable in magnitude to many $W=CH(Ar)$ alkylidene bonds ($1.86–2.15$

Å).³ In addition, this interatomic distance is substantially shorter than the W–C single-bond distance observed in η^1 -vinyl complexes of W (ca. 2.2 Å)⁴ and those of typical $16e$ $Cp^*W(NO)(aryl)_2$ complexes (ca. 2.15 Å).⁵ Indeed, the W–C(11) distance is nearly identical with the W–C contact in a $W(\eta^2-C(O)R)$ acyl fragment,^{5c} a linkage previously described as containing substantial alkylidene character.⁶

Certain structural parameters indicate that the $CPhCH_2$ fragment is bound to the tungsten atom in **1** in a distorted η^2 fashion. For example, the W–C(11)–C(12) bond angle is acute ($97.5(4)^\circ$) yet remains larger than the typical $M=C^1-C^2$ angles observed for other 1-metallacyclopropene complexes ($70–85^\circ$).² The long W–C(12) contact ($2.615(5)$ Å) is greater than a W–C² single bond by a large margin (~ 0.4 Å), and the C(11)–C(12) bond length ($1.342(6)$ Å) is characteristic of a double bond between these centers and is significantly shorter than the distance observed for other 1-metallacyclopropene complexes (~ 1.45 Å). Further evidence for a distortion in this fragment is given by the fact that the vinyl plane embodied by C(12), H(17), and H(16) is tilted by an angle of 25° with respect to the plane defined by W(1), C(11), and C(13). Typical torsion angles observed in the $M=C^1-C^2-R$ fragment for other structurally characterized 1-metallacyclopropene complexes lie in the range of $70–90^\circ$.^{2a,d} The bonding interaction between W and C(12) in **1** is clearly less than that of a W–C single bond. At best, the metal–vinyl interaction observed in the solid-state molecular structure of **1** may be described as a distorted 1-metallacyclopropene unit. The reasons for such a distortion in the solid state are unclear. There exist no unusual intermolecular close contacts in the unit cell that could be responsible for the distortion observed in the 1-metallacyclopropene fragment.

An interesting structural feature that is inconsistent with the assignment of a complete double bond to the C(11)–C(12) link (despite the short bond length associated with this contact) is the angle between the W(1)–C(11) vector and the plane of the phenyl substituent. The two are nearly coplanar: the W(1)–C(11)–C(13)–C(18) torsion angle is $177.9(3)^\circ$, strongly suggesting that the phenyl ring is conjugated with the unsaturation in the W(1)–C(11) link. The analogous torsion angle of $24.1(6)^\circ$ defined by the C(12)–C(11)–C(13)–C(18) chain indicates a reduction in the conjugation between the phenyl ring and the vinyl $C=C$ bond. On the basis of

(2) (a) Allen, S. R.; Beevor, R. G.; Green, M.; Norman, N. C.; Orpen, A. G.; Williams, I. D. *J. Chem. Soc., Dalton Trans.* **1985**, 435. (b) Morrow, J. R.; Tonker, T. L.; Templeton, J. L. *J. Am. Chem. Soc.* **1985**, *107*, 6956. (c) Feng, S. G.; Gamble, A. S.; Templeton, J. L. *Organometallics* **1989**, *8*, 2024. (d) Carfagna, C.; Carr, N.; Deeth, R. J.; Dossett, S. J.; Green, M.; Mahon, M. F.; Vaughan, C. *J. Chem. Soc., Dalton Trans.* **1996**, 415. (e) Allen, S. R.; Green, M.; Orpen, A. G.; Williams, I. D. *J. Chem. Soc., Chem. Commun.* **1982**, 826. (f) Casey, C. P.; Brady, J. T.; Boller, T. M.; Weinhold, F.; Hayashi, R. K. *J. Am. Chem. Soc.* **1998**, *120*, 12500.

(3) Nugent, W. A.; Mayer, J. M. *Metal–Ligand Multiple Bonds*; Wiley: New York, 1988.

(4) van der Zijden, A. A.; Bosch, H. W.; Berke, H. *Organometallics* **1992**, *11*, 563.

(5) (a) Debad, J. D.; Legzdins, P.; Batchelor, R. J.; Einstein, F. W. *Organometallics* **1992**, *11*, 8. (b) Dryden, N. H.; Legzdins, P.; Rettig, S. J.; Veltheer, J. E. *Organometallics* **1992**, *11*, 2583. (c) Debad, J. D.; Legzdins, P.; Batchelor, R. J.; Einstein, W. B. *Organometallics* **1993**, *12*, 2094.

(6) (a) Rusik, C. A.; Collins, M. A.; Gamble, A. S.; Tonker, T. L.; Templeton, J. L. *J. Am. Chem. Soc.* **1989**, *111*, 2550. (b) Feng, S. G.; White, P. S.; Templeton, J. L. *Organometallics* **1993**, *12*, 2131.

Table 1. Numbering Scheme, Yield, and Analytical Data for Complexes 1–7

compd	compd no.	color (yield, ^a %)	anal. found (calcd)		
			C	H	N
Cp*W(NO)(η^2 -CPhCH ₂)(CH ₂ SiMe ₃)	1	burgundy (72)	49.30 (48.98)	6.29 (6.17)	2.52 (2.60)
Cp*W(NO)(η^2 -CPhCH ₂)(Cl)	2	burgundy (74)	44.56 (44.53)	4.49 (4.56)	2.89 (2.87)
Cp*W(NO)(η^1 -CPh=CH ₂)(O ₂ CPh)	3	orange (83)	51.87 (51.37)	4.78 (4.77)	2.60 (2.44)
Cp*W(NO)(η^2 -CPhCH ₂)(OTf)	4	red (58)	37.94 (37.96)	3.70 (3.69)	2.30 (2.33)
Cp*W(NO)(η^1 -CPh=CH ₂)(NH ^t Bu)	5	brown (56)	^b		
Cp*W(NO)(η^2 -CHPhCH ₂ N(C ₃ H ₅) ₂)(Cl)	6	brown (87)	49.43 (49.29)	5.95 (5.69)	4.80 (4.79)
Cp*W(NO)(η^1 -CPh=CH ₂)(H)(PPh ₃)	7	gold (55)	60.68 (60.43)	5.49 (5.75)	2.00 (1.96)
Cp*W(NO)(η^1 -CPh=CH ₂)(D)(PPh ₃)	7-d₁	gold (51)	^c		

^a Isolated yield unless otherwise noted. ^b Satisfactory analysis could not be obtained. ^c Not determined.

this information, assigning double-bond character to both of the W(1)–C(11) and C(11)–C(12) linkages results in an unrealistic hypervalent coordination geometry about C(11). Thus, a more reasonable representation consistent with the observed distortion of the 1-metallacyclopropene unit in the solid state involves the delocalization of electron density throughout the M–C(11)–C(12) fragment (depicted below). For reasons of clarity and consistency, however, this fragment will be represented throughout this report in the form of a 1-metallacyclopropene unit.



In contrast to its solid-state metrical parameters, the solution properties of the vinyl ligand in **1** are distinctly characteristic of a 1-metallacyclopropene group.² For example, the C¹ signal in the ¹³C NMR spectra of **1** is manifested in the alkylidene region (δ 227.9). In addition, the C² signal lies considerably upfield (83.1 ppm), in the region normally associated with metalated, sp³- or sp²-hybridized, σ -bound carbon nuclei in W nitrosyl complexes.^{5c,7} The vinyl proton signals in the ¹H NMR spectrum of **1** likewise appear upfield at 3.88 and 3.56 ppm, near the region normally attributed to the tungsten-bound, alkyl magnetic environment. In addition, the magnitude of the one-bond C _{β} –H coupling constant (¹J_{CH_a} \approx ¹J_{CH_b} \approx 146 Hz) is comparable to those determined for other 1-metallacyclopropene complexes of W.^{2b,c,8}

B. Preparation of Cp*W(NO)(η^2 -CPhCH₂)(X) and Cp*W(NO)(η^1 -CPh=CH₂)(LX) Complexes (X = Cl, OTf; LX = η^2 -O₂CPh, NH^tBu, (PPh₃)(H), (PPh₃)(D)) and Their Solid-State Structural and Solution NMR Spectroscopic Properties. In the ensuing discussion, the synthesis of each new vinyl complex will be considered in turn, along with the relevant structural and spectroscopic data that identify the tungsten-vinyl interaction in each. Analytical data (Table 1), mass spectrometric and infrared spectroscopic data (Table 2), and ¹H and ¹³C NMR spectroscopic data (Table 3) for all compounds discussed in this paper and X-ray crystallographic data (Table 4) for selected compounds are collected in the appropriate tables.

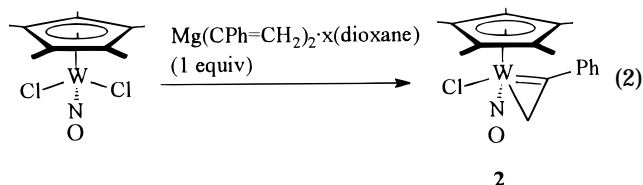
(i) Preparation of Cp*W(NO)(η^2 -CPhCH₂)Cl (2**).** A simple metathesis reaction between the parent dichloride Cp*W(NO)(Cl)₂ and Mg(CPh=CH₂)₂·x(dioxane) (1

Table 2. Mass Spectroscopic and IR Spectral Data for Complexes 1–7

compd no.	MS (<i>m/z</i>) ^a	probe temp ^b (°C)	IR (Nujol, cm ⁻¹)
1	540	180	1539 (ν_{NO})
2	489	150	1580 (ν_{NO})
3	576	120	1574 (ν_{NO}) 1501 (ν_{CO})
4	601	120	1609 (ν_{NO}) 1355 (ν_{SO}) 1237 (ν_{CF})
5	524	200	1588 (ν_{NO})
6	548 ^c	150	1581 (ν_{NO})
7	715	150	1824 (ν_{WH}) 1541 (ν_{NO})
7-d₁	716	150	1543 (ν_{NO}) 1318 (ν_{WD})

^a Values for the highest intensity peak of the calculated isotopic cluster (¹⁸⁴W). ^b Probe temperatures. ^c FAB⁺ mass spectrum.

equiv) at low temperature affords good yields of air-sensitive **2** after workup (eq 2). The identification of the



1-metallacyclopropene fragment in **2** is made on the basis of solution NMR spectroscopic data and its solid-state molecular structure (Figure 2). The ¹H and ¹³C NMR spectra for complex **2** in solution contain signals analogous to those of **1** attributable to the methylene protons (δ 4.43 and 4.25) and the carbenic C¹ (δ 220.8) and alkyl C² (δ 83.6) nuclei of a 1-metallacyclopropene unit. Although the methylene hydrogen atoms were not located in the difference map during refinement of the solid-state crystallographic data, the short W(1)–C(11) contact (2.071(4) Å), the calculated W–C(12) distance of 2.58 Å, the acute W(1)–C(11)–C(12) angle (96.4(3)°), and the expanded W(1)–C(11)–C(13) angle (137.0(3)°) are nearly identical with those of the vinyl ligand in the structure of complex **1** and implicate the presence of a 1-metallacyclopropene unit in the molecular structure of complex **2** analogous to that observed in **1**. Similar to the torsion angle in the solid-state structure of **1**, the respective W(1)–C(11)–C(13)–C(18) angle (170.0(3)°) and the C(12)–C(11)–C(13)–C(18) angle (29.6(6)°) in the solid-state structure of **2** suggests that the phenyl substituent is conjugated both with the carbenic W–C(11) link and the C(11)–C(12) link in the distorted 1-metallacyclopropene fragment.

(7) Legzdins, P.; Rettig, S. J.; Sánchez, L. J. *Organometallics* **1988**, 7, 2394.

(8) Feng, S. G.; Templeton, J. L. *Organometallics* **1992**, 11, 2168.

Table 3. ^1H and ^{13}C NMR Spectroscopic Data for Complexes 1–7

compd no.	^1H NMR ^a (δ /ppm)	^{13}C NMR ^a (δ /ppm)
1^b	7.87 (dd, $^3J_{\text{HH}} = 8.0$ Hz, $^4J_{\text{HH}} = 1.2$ Hz, 2H, Ph H _{ortho})	227.9 (s, $^1J_{\text{WC}} = 99$ Hz, CPhCH ₂)
	7.29 (t, $^3J_{\text{HH}} = 8.0$ Hz, 2H, Ph H _{meta})	145.3 (s, Ph C _{ipso})
	7.11 (t, $^3J_{\text{HH}} = 8.0$ Hz, 1H, Ph H _{para})	129.6 (d, $^1J_{\text{CH}} = 157$ Hz, Ph)
	3.88 (dd, $^2J_{\text{HH}} = 5.4$ Hz, $^5J_{\text{HH}} = 1.2$ Hz, 1H, CPhCH _a H _b)	128.8 (d, $^1J_{\text{CH}} = 157$ Hz, Ph)
	3.56 (dd, $^2J_{\text{HH}} = 5.4$ Hz, $^5J_{\text{HH}} = 1.2$ Hz, 1H, CPhCH _a H _b)	127.6 (d, $^1J_{\text{CH}} = 157$ Hz, Ph)
	1.50 (s, 15H, C ₅ Me ₅)	109.6 (s, C ₅ Me ₅)
	0.69 (d, $^2J_{\text{HH}} = 12.6$ Hz, 1H, CH _a H _b SiMe ₃)	83.1 (dd, $^1J_{\text{CH}_a} \approx ^1J_{\text{CH}_b} \approx 146$ Hz, $^2J_{\text{WC}} = 13$ Hz, CPhCH ₂)
	0.59 (s, 9H, SiMe ₃)	35.5 (t, $^1J_{\text{CH}} = 111$ Hz, CH ₂ SiMe ₃)
	0.21 (d, $^2J_{\text{HH}} = 12.6$ Hz, 1H, CH _a H _b SiMe ₃)	9.5 (q, $^1J_{\text{CH}} = 127$ Hz, C ₅ Me ₅)
		3.4 (q, $^1J_{\text{CH}} = 126$ Hz, CH ₂ SiMe ₃)
2	7.72 (dd, $^3J_{\text{HH}} = 6.0$ Hz, $^4J_{\text{HH}} = 1.2$ Hz, 2H, Ph H _{ortho})	220.8 (CPhCH ₂)
	7.22 (t, $^3J_{\text{HH}} = 6.0$ Hz, 2H, Ph H _{meta})	142.7 (Ph C _{ipso})
	7.13 (t, $^3J_{\text{HH}} = 6.0$ Hz, 1H, Ph H _{para})	129.6, 128.8, 127.6 (Ph)
	4.43 (dd, $^2J_{\text{HH}} = 6.0$ Hz, $^5J_{\text{HH}} = 1.2$ Hz, 1H, CPhCH _a H _b)	112.1 (C ₅ Me ₅)
	4.25 (dd, $^2J_{\text{HH}} = 6.0$ Hz, $^5J_{\text{HH}} = 1.2$ Hz, 1H, CPhCH _a H _b)	83.6 (dd, $^1J_{\text{CH}_a} \approx ^1J_{\text{CH}_b} \approx 151$ Hz, CPhCH ₂)
	1.51 (s, 15H, C ₅ Me ₅)	9.5 (C ₅ Me ₅)
	8.07 (d, $^3J_{\text{HH}} = 7.5$ Hz, 2H, Ph H _{ortho})	189.5 (PhCO ₂)
	7.61 (d, $^3J_{\text{HH}} = 7.8$ Hz, 2H, Ph H _{meta})	179.7 (CPh=CH ₂)
	7.45 (pseudo-t, 4H, Ph H _{meta} , H _{ortho})	151.5 (Ph C _{ipso})
	7.24 (t, $^3J_{\text{HH}} = 6.2$ Hz, 2H, Ph H _{para})	133.8, 130.1, 129.1, 128.4, 128.2, 127.3, 125.5 (Ar)
3	7.12 (t, $^3J_{\text{HH}} = 7.8$ Hz, 1H, Ph H _{para})	122.4 (CPh=CH ₂)
	6.40 (d, $^2J_{\text{HH}} = 2.1$ Hz, 1H, CPh=CH _a H _b)	113.3 (C ₅ Me ₅)
	5.63 (d, $^2J_{\text{HH}} = 2.1$ Hz, 1H, CPh=CH _a H _b)	9.5 (C ₅ Me ₅)
	1.84 (s, 15H, C ₅ Me ₅)	
	7.59 (m, 2H, Ph)	258.0 (CPhCH ₂) ^c
	7.49 (m, 3H, Ph)	140.5 (Ph C _{ipso})
	4.99 (d, $^2J_{\text{HH}} = 8.7$ Hz, $^2J_{\text{WH}} = 3.1$ Hz, 1H, CPhCH _a H _b)	129.1 (Ph C _{ortho})
	4.90 (br d, $^2J_{\text{HH}} = 8.7$ Hz, $^2J_{\text{WH}} = 7.8$ Hz, 1H, CPhCH _a H _b)	128.1, (Ph C _{meta})
	1.98 (s, 15H, C ₅ Me ₅)	125.3 (Ph C _{para})
		119.1 (q, $^1J_{\text{CF}} = 315$ Hz, CF ₃)
4		112.8 (C ₅ Me ₅)
		77.6 (br t, $^1J_{\text{CH}} = 164$ Hz, CPhCH ₂)
		9.6 (q, $^1J_{\text{CH}} = 126$ Hz, CH ₂ SiMe ₃)
		^a 185.1 (CPh=CH ₂)
		150.1 (Ph C _{ipso})
		128.2 (Ph C _{ortho})
		127.7 (Ph C _{meta})
		126.3 (CPh=CH ₂)
		125.6 (Ph C _{para})
		111.6 (s, C ₅ Me ₅)
5	7.77 (br, 1H, NH)	33.4 (HN(CMe ₃))
	7.25 (m, 4H, Ph)	29.7 (HN(CMe ₃))
	7.07 (m, 1H, Ph H _{para})	10.0 (C ₅ Me ₅)
	6.21 (d, $^2J_{\text{HH}} = 3.0$ Hz, 1H, CPh=CH _a H _b)	148.7 (Ph C _{ipso})
	5.51 (d, $^2J_{\text{HH}} = 3.0$ Hz, 1H, CPh=CH _a H _b)	133.6 (NCH ₂ CH=CH ₂)
	1.80 (s, 15H, C ₅ Me ₅)	131.5 (Ph C _{ortho})
	1.39 (s, 9H, 'Bu)	131.1 (NCH ₂ CH=CH ₂)
		128.3 (Ph C _{meta})
		125.2 (Ph C _{para})
		121.6 (NCH ₂ CH=CH ₂)
6	7.69 (d, $^3J_{\text{HH}} = 7.8$ Hz, 2H, Ar H _{ortho})	120.8 (NCH ₂ CH=CH ₂)
	7.29 (t, $^3J_{\text{HH}} = 7.8$ Hz, $^3J_{\text{HH}} = 7.8$ Hz, 2H, Ar H _{meta})	111.3 (C ₅ Me ₅)
	7.03 (t, $^3J_{\text{HH}} = 7.8$ Hz, 1H, Ar H _{para})	64.6 (WCHPhCH ₂)
	6.53 (m, 1H, NCH ₂ CH=CH ₂)	61.0 (NCH ₂ CH=CH ₂)
	5.70 (m, 1H, NCH ₂ CH=CH ₂)	60.8 (NCH ₂ CH=CH ₂)
	5.17 (d, $^3J_{\text{HH}} = 10.2$ Hz, 1H, NCH ₂ CH=CH ₂)	38.9 (WCHPhCH ₂)
	4.90 (m, 3H, NCH ₂ CH=CH ₂ , WCHPhCH ₂)	10.1 (C ₅ Me ₅)
	4.29 (t, $^3J_{\text{HH}} = 12$ Hz, 1H, WCHPhCH ₂)	177.1 (d, $^2J_{\text{PC}} = 21.8$ Hz, CPh=CH ₂)
	4.07 (m, 2H, NCH ₂ CH=CH ₂)	152.9 (Ph C _{ipso})
	3.26 (m, 1H, NCH ₂ CH=CH ₂)	137.2 (d, $^1J_{\text{PC}} = 66$ Hz, Ph C _{ipso})
7^{b,e}	3.00 (m, 1H, NCH ₂ CH=CH ₂)	134.5, 134.2, 129.6, 129.3, 128.8, 128.2 (Ar)
	2.74 (m, 1H, NCH ₂ CH=CH ₂)	125.3 (CPh=CH ₂)
	2.48 (m, 1H, NCH ₂ CH=CH ₂)	106.7 (C ₅ Me ₅)
	1.59 (s, 15H, C ₅ Me ₅)	10.5 (C ₅ Me ₅)
	7.72 (br t, $^3J_{\text{HH}} = 6.8$ Hz, 6H, PPh ₃)	
	7.43 (d, $^3J_{\text{HH}} = 7.2$ Hz, 2H, Ph H _{meta})	
	7.34 (t, $^3J_{\text{HH}} = 7.5$ Hz, 2H, Ph H _{para})	
	7.08 (t, $^3J_{\text{HH}} = 7.5$ Hz, 1H, Ph H _{para})	
	6.98 (m, 9H, PPh ₃)	
	6.31 (d, $^2J_{\text{HH}} = 3.0$ Hz, 1H, CPh=CH _a H _b)	
7-d^b	4.81 (d, $^2J_{\text{HH}} = 3.0$ Hz, 1H, CPh=CH _a H _b)	
	1.71 (s, 15H, C ₅ Me ₅)	
	1.04 (d, $^2J_{\text{PH}} = 96$ Hz, WH)	
	7.72 (br t, $^3J_{\text{HH}} = 6.8$ Hz, 6H, PPh ₃)	<i>f</i>
	7.43 (d, $^3J_{\text{HH}} = 7.2$ Hz, 2H, Ph H _{meta})	
	7.34 (t, $^3J_{\text{HH}} = 7.5$ Hz, 2H, Ph H _{para})	
	7.08 (t, $^3J_{\text{HH}} = 7.5$ Hz, 1H, Ph H _{para})	
	6.98 (m, 9H, PPh ₃)	
	6.31 (d, $^2J_{\text{HH}} = 3.0$ Hz, 1H, CPh=CH _a H _b)	
	4.81 (d, $^2J_{\text{HH}} = 3.0$ Hz, 1H, CPh=CH _a H _b)	
7-d^b	1.71 (s, 15H, C ₅ Me ₅)	

^a ^1H NMR spectra and ^{13}C NMR spectra recorded in CDCl_3 at room temperature unless otherwise noted. ^b ^1H and ^{13}C spectra recorded in C_6D_6 . ^c Spectrum recorded at -70°C in CD_2Cl_2 solvent. ^d Spectrum recorded in acetone- d_6 . ^e ^{31}P NMR spectrum (ref. P(OMe)₃): 27.1 ppm, d, $^2J_{\text{HP}} = 93$ Hz. ^f Not recorded.

Table 4. X-ray Crystallographic Data for Complexes **1**, **2**, **6**, and **7**

	1	2	6	7
Crystal Data				
empirical formula	C ₂₂ H ₃₃ NOSiW	C ₁₈ H ₂₂ ClNOW	C ₂₄ H ₃₃ ClN ₂ OW	C ₃₆ H ₃₈ NOPW
cryst habit, color	prism, burgundy	prism, burgundy	orange, irregular	plate, yellow
cryst size (mm)	0.45 × 0.30 × 0.15	0.12 × 0.30 × 0.40	0.20 × 0.40 × 0.40	0.04 × 0.15 × 0.40
cryst syst	triclinic	triclinic	monoclinic	monoclinic
space group	<i>P</i> 1 (No. 2)	<i>P</i> 1 (No. 2)	<i>C</i> 2 ₁ / <i>c</i> (No. 15)	<i>P</i> 2 ₁ / <i>n</i> (No. 14)
<i>V</i> (Å ³)	1162.0(2)	890.6(2)	4839(1)	6271(1)
<i>a</i> (Å)	8.4119(7)	9.212(1)	29.017(4)	26.039(1)
<i>b</i> (Å)	8.9053(9)	14.235(2)	8.435(2)	8.902(2)
<i>c</i> (Å)	16.717(2)	7.3792(8)	19.812(5)	29.973(1)
α (deg)	89.106(4)	95.72(1)	90	90
β (deg)	87.394(2)	107.674(8)	93.58(2)	115.479(3)
γ (deg)	68.2654(9)	101.38(1)	90	90
<i>Z</i>	2	2	8	8
calcd density (Mg/m ³)	1.542	1.819	1.605	1.515
abs coeff (cm ⁻¹)	49.9	54.6	49.1	75.9
<i>F</i> ₀₀₀	536	472	2320	2864
Data Collection and Refinement				
scan type	ω-2θ	ω-2θ	ω-2θ	ω-2θ
scan width, deg		1.30 + 0.35 tan θ	1.10 + 0.35 tan θ	1.10 + 0.20 tan θ
2θ _{max} , deg	60	70	55.0	155
measd rflns				
total	10 476	8227	6038	13 897
unique	5220 (<i>R</i> _{int} = 0.030)	7824 (<i>R</i> _{int} = 0.034)	5910 (<i>R</i> _{int} = 0.059)	13 609 (<i>R</i> _{int} = 0.064)
corrections	Lorentz-polarizn abs (transmissn factors: 0.4532-1.000)	Lorentz-polarizn abs (transmissn factors: 0.394-1.000)	Lorentz-polarizn abs (transmissn factors: 0.5399-1.000)	Lorentz-polarizn abs (transmissn factors: 0.510-1.000), decay (16.25% decline)
final <i>R</i> indices	<i>R</i> _F = 0.030, <i>R</i> _{wF} = 0.026	<i>R</i> _F = 0.032, <i>R</i> _{wF} = 0.028	<i>R</i> _F = 0.033, <i>R</i> _{wF} = 0.029	<i>R</i> _F = 0.048, <i>R</i> _{wF} = 0.044
goodness of fit on <i>F</i> ²	1.68	1.5	1.33	2.09
largest diff peak and hole (Å ⁻¹)	1.89 and -2.46	1.27 and -1.26	0.56 and -0.68	0.55 and -0.62

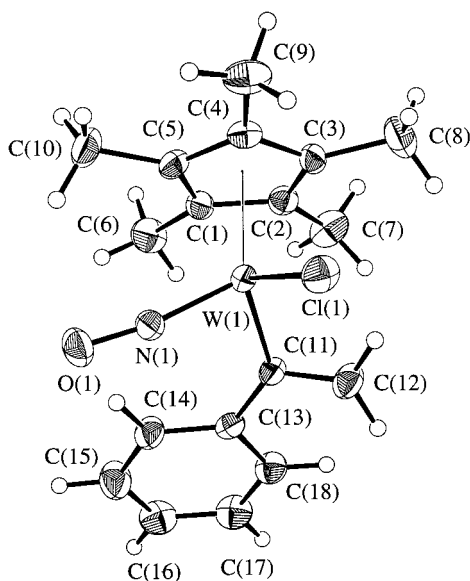
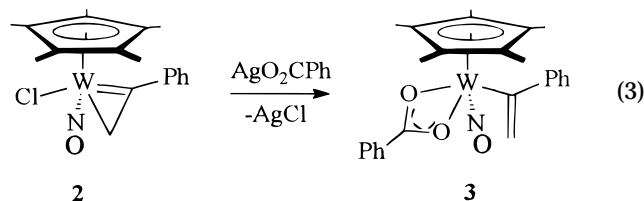


Figure 2. Solid-state molecular structure of **2** with 50% probability thermal ellipsoids depicted. Selected interatomic distances (Å) and angles (deg): W(1)–N(1) = 1.770(3), W(1)–Cp*(centroid) = 2.04, W(1)–Cl(1) = 2.375(1), N(1)–O(1) = 1.214(4), W(1)–C(11) = 2.071(4), C(11)–C(12) = 1.331(6), C(11)–C(13) = 1.469(6); W(1)–C(11)–C(12) = 97.5(4), N(1)–W(1)–C(19) = 96.0(2), C(12)–C(11)–C(13) = 123.0(4), N(1)–W(1)–C(11) = 96.4(3), W(1)–C(11)–C(13) = 137.0(3), Cl(1)–W(1)–N(1) = 99.3(1), Cl(1)–W(1)–Cp*(centroid) = 112.8, Cl(1)–W(1)–C(11) = 115.4(1), C(11)–W(1)–Cp*(centroid) = 113.2, W(1)–N(1)–O(1) = 170.0(3).

(ii) Reaction of Cp*W(NO)(η²-CPhCH₂)Cl (2**) with AgX Salts (X = O₂CPh, OTf).** Silver salts have long been known to abstract halide ligands from Cp*M(NO)-

containing complexes. For example, when such an abstraction is conducted in MeCN utilizing AgBF₄, MeCN-solvated cations are typically isolated.⁹ Similarly, treatment of Cp*M(NO)₂Cl (M = group 6 metal) with AgBF₄ in CH₂Cl₂ generates Cp*M(NO)₂(η¹-BF₄) species which can be used to prepare lactone and pyrone complexes.¹⁰ Not surprisingly, metathesis of the chloride in **2** by AgO₂CPh results in the formation of benzoate-containing **3**, as depicted in eq 3.



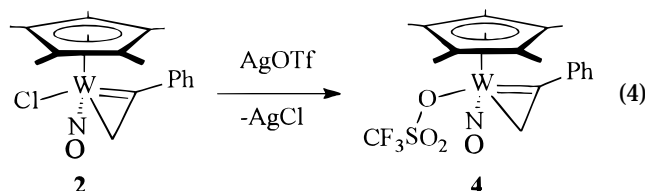
This air-stable compound is isolated as orange needles in good yields by crystallization from diethyl ether. Signals for the vinyl protons in the ¹H NMR spectrum of this compound lie in the alkenyl region of the spectrum at δ 6.40 and 5.63, considerably downfield of the analogous signals for the methylene protons in complexes **1** and **2**. The vinyl C¹ and C² signals appear

(9) (a) Legzdins, P.; Nurse, C. R. *Inorg. Chem.* **1982**, *21*, 3110. (b) Chin, T. T.; Legzdins, P.; Trotter, J.; Yee, V. C. *Organometallics* **1992**, *11*, 913. (c) Legzdins, P.; Rettig, S. J.; Sayers, S. F. *J. Am. Chem. Soc.* **1994**, *116*, 12105. (d) Dryden, N. H.; Legzdins, P.; Sayers, S. F.; Trotter, J.; Yee, V. C. *Can. J. Chem.* **1995**, *73*, 1035. (e) McCleverty, J. A.; Murray, A. J. *Transition Met. Chem.* **1979**, *4*, 273.

(10) (a) Legzdins, P.; Martin, D. T. *Organometallics* **1983**, *2*, 1785. (b) Legzdins, P.; Richter-Addo, G. B.; Einstein, F. W. B.; Jones, R. H. *Organometallics* **1990**, *9*, 431. (c) Legzdins, P.; McNeil, W. S.; Vessey, E. G.; Batchelor, R. J.; Einstein, F. W. B. *Organometallics* **1992**, *11*, 2718.

in the ^{13}C NMR spectrum at δ 179.7 and 122.4, respectively. These data taken together implicate an η^1 -vinyl bonding interaction with the metal center in complex **3**. Thus, the benzoate ligand must coordinate the tungsten center in an η^2 fashion in order to satisfy the electronic saturation at the metal center. The solid-state molecular structure of **3** determined by X-ray crystallography confirms these proposals.¹¹

By analogy to the conversion depicted in eq 2, the reaction of **2** with 1 equiv of AgOTf affords triflate-containing **4** in relatively good yields as a red crystalline solid following workup and crystallization (eq 4). Con-

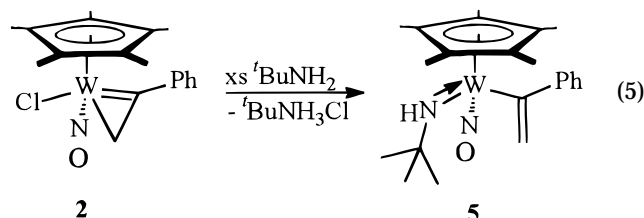


siderable spectroscopic evidence exists in support of the formulation of an inner-sphere triflate ligand in complex **4**. It has been demonstrated previously that the coordination mode of the triflate ligand may be identified from the IR spectrum of the complex in question, the highest energy absorption of the S–O link occurring in the 1200–1280 cm^{-1} range for an ionic triflate group or in the 1300–1380 cm^{-1} range of the IR spectrum for a covalent triflate ligand.¹² Bands attributable to the S–O stretch (1355 cm^{-1}) and C–F stretch (1237 cm^{-1}) of a covalently bound triflate ligand are evident in the IR Nujol mull spectrum of complex **4**. In addition, ν_{NO} occurs at 1609 cm^{-1} in the region normally associated with electroneutral organometallic nitrosyl complexes,¹³ a further indication of a covalently bound triflate ligand in solid-state **4**.

While it is conceivable that the covalent triflate ligand could bind to W in a bidentate fashion to afford an 18e complex analogous to benzoate-containing **3**, the solution NMR data obtained for **4** are inconsistent with the requisite η^1 -vinyl bonding interaction that would also result. The signals attributable to the 1-metallacyclopropene C^1 and C^2 nuclei appear at 258.0 and 77.6 ppm, respectively, in the ^{13}C NMR spectrum of **4**, and the methylene proton signals appear in the ^1H NMR spectrum for **4** at 4.90 and 4.99 ppm. Interestingly, the upfield vinyl H signal is broadened and lower in intensity than the downfield signal, suggestive of a fluxional process or an interatomic interaction involving one of the vinyl hydrogen atoms and either the metal center or an atom of the triflate ligand. The broadened signal attributable to the C^2 resonance in the $^{13}\text{C}\{^1\text{H}\}$ NMR spectrum of **4** exists as a broad pseudo-triplet ($^1J_{\text{CH}_a} \approx ^1J_{\text{CH}_b} \approx 164$ Hz) in the gate-decoupled $^{13}\text{C}\{^1\text{H}\}$ NMR spectrum. On the basis of these NMR spectroscopic data it can be concluded that the vinyl fragment in **4** is bound to tungsten as a component of a 1-metallacyclopropene unit, as established for complexes **1** and **2**. The nature of the fluxional process that broadens the metallacyclopropene H and C signals in the NMR

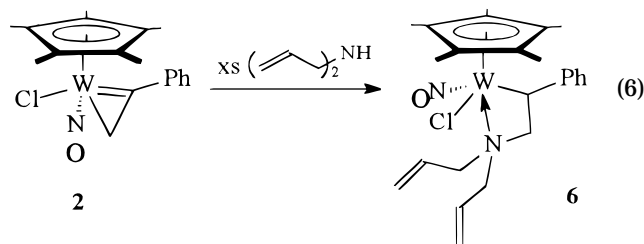
spectra of **4** remains uncertain, though variable-temperature ^1H NMR experiments reveal that this interaction is temperature dependent.

(iii) **Reaction of 2 with Excess $t\text{BuNH}_2$ and $(\text{C}_3\text{H}_5)_2\text{NH}$.** A common method used to introduce an amide ligand into an organometallic complex involves the reaction of excess amine with an organometallic halide in an aminolysis reaction.¹⁴ Two equivalents of amine is consumed in this reaction as the halide is eliminated from the organometallic complex as the counteranion in an ammonium salt. The reaction of chloride-containing **2** with excess $t\text{BuNH}_2$ in this way affords amide-containing **5** in moderate yields as yellow microcrystals (eq 5).¹⁵ The amine H resonance of **5** is



observed as a broad singlet at 7.77 ppm in the ^1H NMR spectrum, and the *tert*-butyl group is evidenced by an intense singlet that integrates for 9 H at 1.39 ppm. Analogous to the NMR signals observed for benzoate-containing **3**, the chemical shifts of the ^1H and ^{13}C resonances attributable to the respective vinyl protons (6.21 and 5.51 ppm) and the vinyl carbon nuclei in **5** (185.1 and 126.3 ppm for C^1 and C^2 , respectively) are indicative of an η^1 -vinyl bonding interaction with W.

Interestingly, exposure of **2** to an excess of diallylamine does not yield the corresponding secondary amide vinyl complex. Instead, an unusual product of the coupling of vinyl and amine fragments is formed in high yield (complex **6**, eq 6). The solid-state molecular



structure determined for this complex, depicted in Figure 3, reveals that the chloride ligand remains in the coordination sphere of tungsten. In addition, the diallylamine unit is bound to W via a dative bond ($\text{W}(1)–\text{N}(1) = 2.310(6)$ Å) and to the vinyl fragment through a single N–C bond ($\text{N}(1)–\text{C}(11) = 1.491(8)$ Å) as a component of an azametallacyclobutane ring.¹⁶ The $\text{C}(11)–\text{C}(12)$ contact (1.51(1) Å) and the $\text{W}(1)–\text{C}(12)$

(14) See: Legzdins, P.; Rettig, S. J.; Ross, K. J. *Organometallics* **1993**, *12*, 2103 and references therein.

(15) Satisfactory analysis could not be obtained for this complex. It has been suggested by the microanalyst that the formation of tungsten nitrides during combustion can lead to a reduction in the observed carbon and nitrogen analyses.

(16) For another example of a W nitrosyl complex containing both a W–N dative bond and C–N single bond, see: Debad, J. D.; Legzdins, P.; Lumb, S. A.; Batchelor, R. J.; Einstein, F. W. B. *Organometallics* **1995**, *14*, 2543.

(11) Einstein, F. W. B.; Batchelor, R. J. Unpublished observations.

(12) (a) Lawrence, G. A. *Chem. Rev.* **1986**, *86*, 17. (b) Otieno, T.; Rettig, S. J.; Thompson, R. J.; Trotter, J. *Can. J. Chem.* **1990**, *68*, 1901.

(13) Richter-Addo, G. B.; Legzdins, P. *Metal Nitrosyls*; Oxford University Press: New York, 1992.

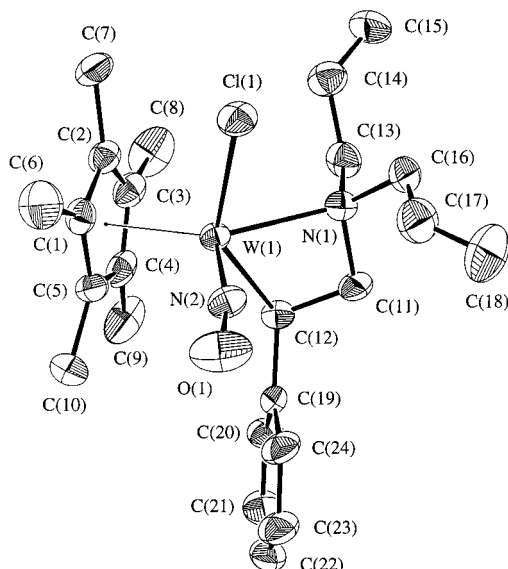
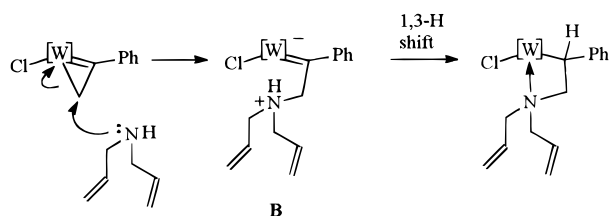


Figure 3. Solid-state molecular structure of **6** with 50% probability thermal ellipsoids depicted. Selected interatomic distances (Å) and angles (deg): W(1)–N(2) = 1.747(6), W(1)–Cp*(centroid) = 2.06, N(2)–O(1) = 1.227(7), W(1)–N(1) = 2.310(6), W(1)–Cl(1) = 2.451(2), W(1)–C(12) = 2.255(7), C(11)–C(12) = 1.51(1), C(11)–N(1) = 1.491(8); W(1)–C(12)–C(11) = 92.7(4), N(2)–W(1)–C(12) = 92.4(3), Cl(1)–W(1)–N(1) = 79.2(2), Cl(1)–W(1)–N(2) = 90.2(2), C(11)–C(12)–C(119) = 112.5(6), C(12)–C(11)–N(1) = 103.6(6), N(1)–W(1)–C(12) = 62.3(2), C(12)–W(1)–Cp*(centroid) = 107.1, W(1)–N(2)–O(1) = 168.4(7), N(1)–W(1)–Cp*(centroid) = 139.7, N(2)–W(1)–Cp*(centroid) = 117.6, C(13)–N(1)–C(16) = 106.9(6).

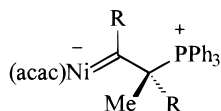
Scheme 1



distance (2.255(7) Å) are those of typical C–C and W–C single bonds.¹⁷

A reasonable mechanistic pathway for this transformation is shown in Scheme 1. Attack at the methylene carbon by diallylamine affords a zwitterionic ammonium alkylidene complex which, upon tautomerization and coordination of the pendant amine, leads to the formation of **6**.

Support for this pathway is provided by Bergman's report of an isolable zwitterionic phosphonium carbene complex.¹⁸



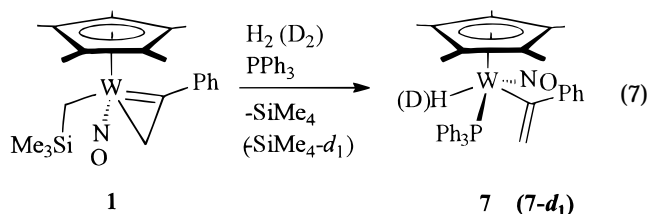
Intermediate B depicted in Scheme 1 is an analogue to this phosphonium carbene complex, and the formation

of **6** logically extends from the intermediacy of such a tungsten carbene complex via amine–H tautomerization.

It is interesting that the reaction of **2** with diallylamine does not yield the desired amide vinyl complex, whereas the reaction of *tert*-butylamine with **2** does. It is possible that the difference in the reactivity of *tert*-butylamine and diallylamine with complex **2** could be due to a difference in the steric profile of the two reagents. The coordination environment about W in complex **2** is considerably congested due to the presence of the 1-metallacyclopentene unit, and as a result, its accessibility to incoming reagents is presumably determined by the steric demands of the reagent. *tert*-Butylamine is a primary amine and has a smaller steric cross-section than does the secondary diallylamine reagent. Thus, attack at the metal center by the diallylamine reagent is hindered and the preferred site of reactivity is at the kinetically more accessible metallacyclopentene unit.

(iv) Synthesis and Properties of Cp*W(NO)(η^1 -CPh=CH₂)(H)(PPh₃) (7**).** Complexes of the form Cp*M(NO)(R)₂ (M = Mo, W; R = hydrocarbyl) are known to be Lewis acidic at the metal center and undergo reactions with a variety of electron-rich small molecules. In particular, the reaction of Cp*W(NO)(CH₂SiMe₃)₂ with H₂ has been investigated in great detail. At high pressures of dihydrogen, bimetallic tetrahydride complexes of tungsten are obtained in high yields following the extrusion of 2 equiv of SiMe₄.¹⁹ On the other hand, the reaction of Cp*W(NO)(CH₂SiMe₃)₂ with dihydrogen at low pressures leads to the extrusion of only 1 equiv of SiMe₄.¹⁹ The hydride-containing species Cp*W(NO)-(CH₂SiMe₃)(H) that is transiently generated undergoes a variety of hydrotungstenation reactions in the presence of unsaturated substrates²⁰ and can be trapped as an 18e adduct by PMe₃.¹⁹

The analogous reaction of Cp*W(NO)(CH₂SiMe₃)(η^2 -CPh=CH₂) (**1**) with H₂ in the presence of PPh₃ affords the air-sensitive, ether-soluble vinyl hydride **7** (eq 7).



The presence of a hydride ligand in **7** is made obvious by the medium-intensity W–H stretch evident in the IR Nujol mull spectrum (1824 cm^{−1}) and by the hydride resonance in the ¹H NMR spectrum (δ 1.04, ²J_{PH} = 96.1 Hz) of **7**. These signals appear in the same regions of their respective spectra as those of other phosphine-containing nitrosyl hydride complexes of tungsten.²¹ The deuteride-containing **7-d₁** may be prepared analogously in the presence of D₂ gas. Evidence for the presence of a deuteride ligand in **7-d₁** is given by a W–D stretch in its IR Nujol mull spectrum (1318 cm^{−1}) that is shifted

(19) Legzdins, P.; Martin, J. T.; Einstein, F. W. B.; Jones, R. H. *Organometallics* **1987**, *6*, 1826.

(20) Debad, J. D.; Legzdins, P.; Lumb, S. A.; Batchelor, R. J.; Einstein, F. W. B. *Organometallics* **1995**, *14*, 2543.

(21) Martin, J. T. Ph.D. Thesis, The University of British Columbia, 1987.

(17) See, for example: Debad, J. D.; Legzdins, P.; Rettig, S. J.; Veltheer, J. E. *Organometallics* **1993**, *12*, 2714.

(18) Huggins, J. M.; Bergman, R. G. *J. Am. Chem. Soc.* **1979**, *101*, 4410.

Table 5. ^{13}C NMR Spectroscopic and Solid-State Structural Parameters for the Vinyl Ligand in 1-Metallacyclopropene and η^1 -Vinyl Complexes

complex	vinyl ^{13}C NMR Data		vinyl ligand solid-state structural params		
	$\delta(\text{C}_\alpha)$	$\delta(\text{C}_\beta)$	$d(\text{M}-\text{C}_\alpha)$, Å	$d(\text{M}-\text{C}_\beta)$, Å	$\angle(\text{M}-\text{C}_\alpha-\text{C}_\beta)$, deg
1-Metallacyclopropene Complexes					
$(\eta^5\text{-C}_9\text{H}_7)\text{Mo}(\eta^2\text{-C}(\text{SiMe}_3)\text{CH}_2)(\text{P}(\text{OMe})_3)^a$	276.5 ^b	28.9 ^b	1.957(3)	2.260(4)	82.0(2)
$(\text{Me}_2\text{NCS}_2)_3\text{W}(\eta^2\text{-CPhCPhCPh=CHPh})^c$	260.6 ^d	62.1 ^d	1.94(1)	2.32(1)	85.5(4)
$\text{Cp}^*\text{W}(\text{NO})(\eta^2\text{-CPhCH}_2)(\text{OTf})$ (4) ^e	258.0 ^f	77.6 ^f			
$\text{Cp}^*\text{W}(\text{NO})(\eta^2\text{-CPhCH}_2)(\text{CH}_2\text{SiMe}_3)$ (1) ^e	227.9 ^g	83.1 ^g	2.076(5)	2.615(5)	97.5(4)
$\text{Cp}^*\text{W}(\text{NO})(\eta^2\text{-CPhCH}_2)(\text{Cl})$ (2) ^e	220.8 ^f	83.6 ^f	2.071(4)	2.58 ^h	96.4(3)
η^1-Vinyl Complexes					
$\text{Cp}^*\text{W}(\text{NO})(\eta^1\text{-CPh=CH}_2)(\text{NHtBu})$ (5) ^e	185.1 ^f	126.3 ^f			
$\text{Cp}^*\text{W}(\text{NO})(\eta^1\text{-CPh=CH}_2)(\eta^2\text{-O}_2\text{CPh})$ (3) ^e	179.7 ^f	122.4 ^f			
$\text{Cp}^*\text{W}(\text{NO})(\eta^1\text{-CPh=CH}_2)(\text{H})(\text{PPh}_3)$ (7) ^e	177.1 ^b	125.3 ^b	2.21(1)	3.10 ^h	120(1)

^a Reference 2e. ^b Spectrum recorded in C_6D_6 . ^c Reference 2c. ^d Spectrum recorded in toluene- d_8 . ^e This work. ^f Spectrum recorded in CDCl_3 . ^g Spectrum recorded in CD_2Cl_2 . ^h Calculated distance.

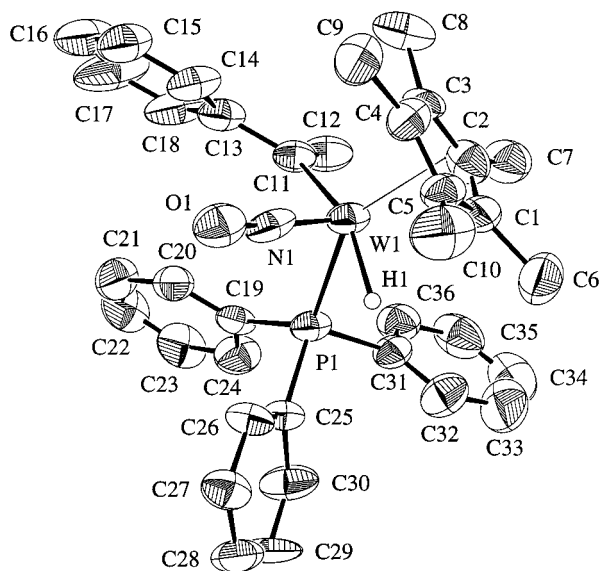


Figure 4. Solid-state molecular structure of **7** with 50% probability thermal ellipsoids depicted. Selected interatomic distances (Å) and angles (deg): $\text{W}(1)-\text{N}(1) = 1.66(2)$, $\text{W}(1)-\text{Cp}^*(\text{centroid}) = 2.04$, $\text{W}(1)-\text{P}(1) = 2.519(3)$, $\text{W}(1)-\text{H}(1) = 1.73$, $\text{N}(1)-\text{O}(1) = 1.28(2)$, $\text{W}(1)-\text{C}(11) = 2.21(1)$, $\text{C}(11)-\text{C}(12) = 1.33(2)$, $\text{C}(11)-\text{C}(13) = 1.52(2)$; $\text{P}(1)-\text{W}(1)-\text{N}(1) = 95.1(4)$, $\text{P}(1)-\text{W}(1)-\text{Cp}^*(\text{centroid}) = 141.4$, $\text{N}(1)-\text{W}(1)-\text{Cp}^*(\text{centroid}) = 118.7$, $\text{W}(1)-\text{C}(11)-\text{C}(12) = 120(1)$, $\text{C}(12)-\text{C}(11)-\text{C}(13) = 116(1)$, $\text{N}(1)-\text{W}(1)-\text{C}(11) = 98.2(6)$, $\text{W}(1)-\text{C}(11)-\text{C}(13) = 123(1)$, $\text{C}(11)-\text{W}(1)-\text{Cp}^*(\text{centroid}) = 109.1$, $\text{W}(1)-\text{N}(1)-\text{O}(1) = 166(1)$, $\text{P}(1)-\text{W}(1)-\text{C}(11) = 81.5(3)$, $\text{P}(1)-\text{W}(1)-\text{H}(1) = 75.4$, $\text{C}(11)-\text{W}(1)-\text{H}(1) = 156.1$, $\text{N}(1)-\text{W}(1)-\text{H}(1) = 78.4$, $\text{H}(1)-\text{W}(1)-\text{Cp}^*(\text{centroid}) = 92.9$.

relative to the $\text{W}-\text{H}$ stretch in **7**. The magnitude of this value is in good agreement with the expected theoretical value of 1290 cm^{-1} .²² The signals in the ^1H and ^{13}C NMR spectra attributable to the vinyl ligand in these complexes are characteristic of an η^1 -vinyl ligand. The vinyl protons resonate at 6.31 and 4.81 ppm, and the C^1 and C^2 signals are identified in the olefinic region at 177.1 and 125.3 ppm, respectively.

(22) This calculation is based upon the assumption that the ground-state vibrational frequency of an $\text{X}-\text{H}$ bond will have the frequency $\nu = 1/2\pi(K/\mu)^{1/2}$, based on the simple harmonic oscillator model, where K is the force constant and μ = reduced mass = $m_{\text{X}}m_{\text{H}}/(m_{\text{X}} + m_{\text{H}})$. If $m_{\text{X}} \gg m_{\text{H}}$, then $\mu \approx m_{\text{H}}$. Making the same argument for an $\text{X}-\text{D}$ bond, and assuming that $\mu_{\text{H}} \approx m_{\text{H}}$, $\mu_{\text{D}} \approx m_{\text{D}}$, and $K_{\text{H}} \approx K_{\text{D}}$, then $\nu_{\text{H}}/\nu_{\text{D}} = (m_{\text{D}}/m_{\text{H}})^{1/2} = 2^{1/2}$. For a more detailed analysis, see: Connors, K. A. *Chemical Kinetics*; VCH: New York, 1990.

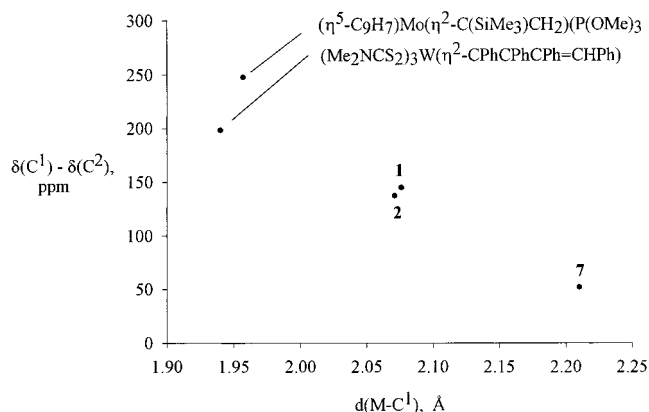


Figure 5. Correlation of $\delta(\text{C}^1) - \delta(\text{C}^2)$ and the solid-state $\text{M}=\text{C}^1$ distance.

The existence of a hydride ligand in complex **7** is confirmed by its solid-state molecular structure (Figure 4), the hydride ligand having been located in the difference map. The $\text{W}(1)-\text{H}(1)$ distance (1.73 Å) and $\text{W}(1)-\text{P}(1)$ distance (2.519(3) Å) are comparable to those of other structurally characterized phosphine-trapped hydride complexes of the $\text{Cp}^*\text{W}(\text{NO})$ fragment.^{19,21} The vinyl ligand's metrical parameters are clearly characteristic of an η^1 -vinyl ligand. For example, the $\text{W}(1)-\text{C}(11)$ bond distance (2.21 Å) is that of a single $\text{W}-\text{C}$ bond. Likewise, the calculated $\text{W}-\text{C}(12)$ distance of 3.10 Å is greater than the sum of the van der Waals radii of the two nuclei. In addition, the $\text{W}(1)-\text{C}(11)-\text{C}(12)$ bond angle of $120(1)^\circ$, the $\text{W}(1)-\text{C}(11)-\text{C}(13)$ angle of $123(1)^\circ$, and the $\text{C}(11)-\text{C}(12)$ bond length of $1.33(2)$ Å are indicative of sp^2 hybridization at $\text{C}(11)$ and double-bond character in the $\text{C}(11)-\text{C}(12)$ contact.

C. NMR Spectroscopic and Solid-State Metrical Correlations for η^1 -Vinyl and 1-Metallacyclopropene Complexes. A comparison of the NMR spectroscopic parameters of the metallacyclopropene units in the complexes **1**, **2**, and **4** to those of known 1-metallacyclopropene complexes and η^1 -vinyl complexes reveals that the physical characteristics of the 1-metallacyclopropene units in **1**, **2**, and **4** lie intermediate between those of the pure 1-metallacyclopropene and η^1 -vinyl limiting forms (Table 5). In addition, graphical correlations between the chemical shift difference of the two carbon nuclei in the vinyl fragment, $\delta(\text{C}^1) - \delta(\text{C}^2)$, and the solid-state $\text{M}=\text{C}^1$ distance (Figure 5) and $\text{M}=\text{C}^1-\text{C}^2$ angle (Figure 6) also indicate that the physical

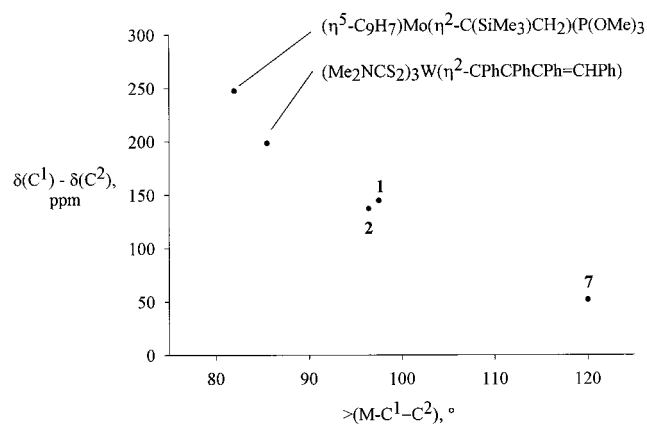


Figure 6. Correlation of $\delta(\text{C}^1) - \delta(\text{C}^2)$ and the solid-state $\text{M}=\text{C}^1-\text{C}^2$ angle.

attributes of the vinyl fragment in **1** and **2** lie closer to, yet less than, those of the pure 1-metallacyclopropene form. Clearly, a 1-metallacyclopropene fragment is typified by signals in the ^{13}C NMR spectrum at low and high field attributable to the alkylidene and alkyl carbon nuclei, respectively, whereas the C^1 and C^2 signals of the η^1 -vinyl ligand appear mid-spectrum (120–190 ppm). The alkylidene carbon signals for the 1-metallacyclopropene units in **1** and **2** are carbenic in character, and the C^2 signals appear upfield in the region associated with metalated paraffinic carbon resonances in $\text{Cp}^*\text{W}(\text{NO})$ -containing hydrocarbyl complexes.^{5c,14,23} The tungsten–vinyl contacts and the metal–vinyl angles determined for these complexes in the solid state are intermediate between those typically observed for the two limiting bonding forms. In particular, the long $\text{W}-\text{C}_\beta$ bonding interactions and the expanded $\text{W}-\text{C}^1-\text{C}^2$ angles in **1** and **2** suggest that the $\text{W}-\text{C}^2$ contact is less than that of a $\text{W}-\text{C}$ single bond in the solid-state structures of these compounds.

The hapticity of the tungsten–vinyl interaction is clearly dependent upon the donor ability of the other X or LX ligands in the coordination sphere of tungsten ($\text{X} = \text{CH}_2\text{SiMe}_3$, Cl, OTf; $\text{LX} = \text{O}_2\text{CPh}$, NH^tBu , $(\text{PPh}_3)(\text{H})$). Thus, conclusions regarding the relative electron-donor ability of the vinyl ligand and a particular X or LX ligand may be made on the basis of the nature of the tungsten–vinyl interaction that is manifested in each of these complexes. For example, each of the X ligands in complexes **1**, **2**, and **4** possesses the capacity to function as a 3e LX ligand: the neosilyl ligand in **1** via an $\alpha\text{-C}-\text{H}$ agostic interaction, the chloride ligand in **2** via π -donation of p(lone pair) electron density, and the triflate ligand in **4** via η^2 coordination of two of the sulfonate oxygen atoms. However, the vinyl ligand is a stronger electron donor than any of these X ligands, and a distorted 3e 1-metallacyclopropene link is detected in these compounds. In contrast, the respective benzoate and amide ligands in complexes **3** and **5** are stronger electron donors relative to the vinyl ligand. As a result, the vinyl ligand is forced to assume the η^1 bonding mode to avoid an expansion of the tungsten valence shell to 20e.

Conclusions

Several 1-metallacyclopropene and η^1 -vinyl-containing complexes have been synthesized, and their solution NMR spectroscopic and solid-state metrical parameters have been investigated and compared to those of complexes reported in the literature that also contain these types of ligands. The results of these comparisons imply that the vinyl ligands in complexes **1**, **2**, and **4** exist in a form best described as a distorted 1-metallacyclopropene unit. While the solution NMR spectroscopic properties observed for this fragment in complexes **1**, **2**, and **4** are more closely allied to those of previously reported 1-metallacyclopropene complexes, the solid-state structural properties of this fragment in complexes **1** and **2** are intermediate between those of other structurally characterized 1-metallacyclopropene complexes and η^1 -vinyl complexes reported in the literature.

The donor ability of the CPhCH_2 ligand in these $\text{Cp}^*\text{W}(\text{NO})$ -containing complexes can be assessed on the basis of the bonding that is assumed in this fragment in response to the presence of other X or LX ligands in the tungsten coordination sphere. Pure σ -donor ligands such as hydrocarbyls and weak π -donor ligands such as chloride and triflate allow the stronger donor CPhCH_2 fragment to assume the 1-metallacyclopropene form. Strong donor ligands such as benzoate and amide force the vinyl ligand into the η^1 form to avoid an expansion of the tungsten valence shell to 20e.

Experimental Section

General Methods. All reactions and subsequent manipulations were performed under anaerobic and anhydrous conditions under either high vacuum or an atmosphere of dinitrogen or argon. General procedures routinely employed in these laboratories have been described in detail previously.²⁴ The organometallic reagents, namely $\text{Cp}^*\text{W}(\text{NO})(\text{Cl})_2$,^{4b} $\text{Cp}^*\text{W}(\text{NO})(\text{CH}_2\text{SiMe}_3)(\eta^2\text{-CPhCH}_2)$,¹ and $\text{Mg}(\text{CPh}=\text{CH}_2)_2 \cdot x(\text{dioxane})$ ²⁵ were prepared according to published procedures. H_2 (Linde, extra dry) and D_2 (CIL) were used as received. PPh_3 (Aldrich) was recrystallized from hexanes. $t\text{BuNH}_2$ (Aldrich) and $(\text{C}_3\text{H}_5)_2\text{NH}$ (Aldrich) were dried over CaH_2 and vacuum-transferred as required. AgO_2CPh (Aldrich) and AgOTf (Aldrich) were stored under dinitrogen in the glovebox and used as supplied without further purification.

X-ray Crystallographic Studies. Data collection and structure solution for complexes **1**, **2**, **6**, and **7** was conducted at the University of British Columbia. Measurements for complex **1** were recorded on a Rigaku/ADSC diffractometer equipped with a CCD area detector. Data collection for complexes **2**, **6**, and **7** were recorded on a Rigaku AFC 63 diffractometer. In all cases, the samples were irradiated with graphite-monochromated Mo K α radiation ($\lambda = 0.71069 \text{ \AA}$). All four structures were solved by heavy-atom Patterson methods and expanded using Fourier techniques. For complex **1**, all of the hydrogen atoms were located in the difference map, though only the vinyl hydrogens (H(16) and H(17)) were refined isotropically. The remainder were included in idealized positions with $d(\text{C}-\text{H}) = 0.98 \text{ \AA}$. Hydrogen atoms in the structures determined for complexes **2**, **6**, and **7** were fixed in calculated positions with $d(\text{C}-\text{H}) = 0.98 \text{ \AA}$, except for the hydride ligand in **7**, which was fixed in the difference map position and refined isotropically. Two crystallographically independent molecules of **7** were identified in the crystal

(23) (a) Dryden, N. H.; Legzdins, P.; Trotter, J. Yee, V. C. *Organometallics* **1991**, *10*, 2857. (b) Dryden, N. H.; Legzdins, P.; Lundmark, P. J. *Organometallics* **1993**, *12*, 2085.

(24) Legzdins, P.; Rettig, S. J.; Ross, K. J.; Batchelor, R. J.; Einstein, F. W. B. *Organometallics* **1995**, *14*, 5579.

(25) Dryden, N. H.; Legzdins, P.; Batchelor, R. J.; Einstein, F. W. B. *Organometallics* **1991**, *10*, 2077.

lattice. The vinyl ligand in one of the two molecules shows evidence of disorder; however, no attempt to model the disorder was made. All calculations were performed using the teXsan²⁶ crystallographic software package of Molecular Structure Corp.

Preparation of $\text{Cp}^*\text{W}(\text{NO})(\eta^2\text{-CPhCH}_2)(\text{Cl})$ (2**).** Brown, powdery $\text{Cp}^*\text{W}(\text{NO})(\text{Cl})_2$ (420 mg, 1 mmol) and white solid $\text{Mg}(\text{CPh}=\text{CH}_2)_2 \cdot x(\text{dioxane})$ (105 mg, 1 equiv) were placed in a 50 mL Erlenmeyer flask in an inert-atmosphere glovebox. The flask was cooled to $\sim -100^\circ\text{C}$ in a liquid- N_2 -cooled cold well over 20 min. THF (10 mL) was placed in a stoppered vial and precooled to -35°C in the glovebox freezer. The contents of the THF vial were pipetted down the walls of the Erlenmeyer flask submerged in the cold well, forming a solid puck of THF on top of the solids in the base of the flask. The reaction flask was then placed on a rotary evaporator. Warming the mixture slowly to room temperature was accompanied by a color change to a deep burgundy-black. After this mixture was stirred at room temperature for 15 min, the THF was removed from the final reaction mixture under vacuum to leave a burgundy-brown solid. The solid was washed with diethyl ether (3×2 mL) and then dried under high vacuum for another 5 min. Methylene chloride was added (7 mL), and the resulting burgundy suspension was filtered through Celite. The filtrate was concentrated, hexanes were added (3 mL), and the burgundy solution was placed in the freezer (-35°C) overnight to induce the crystallization of pure **2** as burgundy blocks (280 mg). Concentration and cooling of the mother liquor to -35°C overnight afforded a second crop of crystals (80 mg).

Preparation of $\text{Cp}^*\text{W}(\text{NO})(\eta^1\text{-CPh}=\text{CH}_2)(\eta^2\text{-O}_2\text{CPh})$ (3**).** Burgundy **2** (244 mg, 0.5 mmol) was dissolved in CH_2Cl_2 (8 mL) in a 25-mL Erlenmeyer flask in an inert-atmosphere glovebox. AgO_2CPh (115 mg, 1 equiv) was placed in a stoppered vial and suspended in CH_2Cl_2 . The flask and vial were both cooled to -35°C in the glovebox freezer. After 15 min the two vessels were removed from the freezer and the contents of the vial were slowly added to the Erlenmeyer flask. As the mixture was warmed to room temperature, a color change to dark orange and the formation of a flocculent white precipitate occurred. After being stirred at room temperature for 15 min, the solvent was removed from the final reaction mixture under vacuum to leave an orange residue. Diethyl ether (20 mL) was added, and the resulting orange suspension was filtered through Celite. The orange filtrate was concentrated, hexanes (2 mL) were added, and the solution was placed in a freezer (-35°C) overnight to induce the crystallization of pure **3** as orange needles (172 mg). Concentration and cooling of the mother liquor to -35°C overnight afforded a second crop of crystals (66 mg).

Preparation of $\text{Cp}^*\text{W}(\text{NO})(\eta^2\text{-CPhCH}_2)(\text{OTf})$ (4**).** Complex **4** was prepared by the reaction of complex **2** (244 mg, 0.5 mmol) and AgOTf (129 mg, 1 equiv) in a manner analogous to the preparation of complex **3**, except that the AgOTf was dissolved in diethyl ether (3 mL). An identical workup procedure resulted in the precipitation of pure **4** as a red microcrystalline solid (175 mg).

Preparation of $\text{Cp}^*\text{W}(\text{NO})(\eta^1\text{-CPh}=\text{CH}_2)(\text{NH}^t\text{Bu})$ (5**).** Crystalline **2** (244 mg, 0.5 mmol) was dissolved in THF (7 mL) in a Schlenk tube. The tube was connected to a vacuum-transfer bridge and cooled to -196°C in a liquid- N_2 bath. $^t\text{BuNH}_2$ (excess) was vacuum-transferred onto the resulting frozen solution. The mixture was warmed to room temperature with stirring, whereupon a color change to brown occurred. After being stirred at room temperature for 15 min, the solvent was removed from the final reaction mixture under vacuum to leave a yellow-brown residue. Methylene chloride/hexanes (1:2, 5 mL) was added, and the resulting suspension was filtered through Celite. The yellow filtrate was concentrated, hexanes (3 mL) were added, and the solution was placed in a freezer (-35°C) overnight to induce the precipitation of **5** as a yellow-brown, microcrystalline aggregate (148 mg).

Preparation of $\text{Cp}^*\text{W}(\text{NO})(\eta^2\text{-CHPhCH}_2\text{N}(\text{C}_3\text{H}_5)_2)(\text{Cl})$ (6**).** Complex **6** was prepared in a manner analogous to **5** except that excess diallylamine was vacuum-transferred onto the solid solution of complex **2**. An identical workup procedure afforded large prismatic crystals of pure **6** (254 g) after the brown filtrate was kept at -35°C for 3 days in the glovebox freezer.

Preparation of $\text{Cp}^*\text{W}(\text{NO})(\eta^1\text{-CPh}=\text{CH}_2)(\text{H})(\text{PPh}_3)$ (7**).** $\text{Cp}^*\text{W}(\text{NO})(\text{CPh}=\text{CH}_2)(\text{CH}_2\text{SiMe}_3)$ (135 mg, 0.25 mmol) and PPh_3 (66 mg, 1 equiv) were dissolved in hexanes (20 mL) in a thick-walled glass reaction bomb. The bomb was connected to a cylinder of H_2 and frozen in a liquid-nitrogen bath. The bomb was submitted to three freeze-pump-thaw cycles, whereupon after the third evacuation dihydrogen (14 psig) was added. The bomb was then maintained at 0°C in a constant-temperature bath for 4 days, during which time gold needles of **7** deposited on the walls of the flask. After 4 days the H_2 was removed under vacuum and the mother liquor was decanted from the crystals. The bomb was evacuated and left under vacuum for 1 h, after which time the gold crystals were isolated (58 mg). The mother liquor was concentrated and cooled in a freezer to induce further precipitation of **7** as an analytically pure straw yellow powder (40 mg).

Preparation of $\text{Cp}^*\text{W}(\text{NO})(\eta^1\text{-CPh}=\text{CH}_2)(\text{D})(\text{PPh}_3)$ (7-d**).** Complex **7-d** was prepared in a manner analogous to complex **7** except that D_2 was employed in the place of H_2 . An identical workup procedure afforded gold **7-d** (90 mg).

Acknowledgment. We are grateful to the Natural Sciences and Engineering Research Council of Canada for support of this work in the form of grants to P.L. and a postgraduate fellowship to S.A.L. We also thank The University of British Columbia for the award of a University Graduate Fellowship to S.A.L.

Supporting Information Available: Tables listing crystallographic information, atomic coordinates and B_{eq} values, anisotropic thermal parameters, and intramolecular bond distances, angles, and torsion angles. This material is available free of charge via the Internet at <http://pubs.acs.org>.

OM990178Y

(26) teXsan Crystal Structure Analysis Package; Molecular Structure Corp., The Woodlands, TX, 1985, 1992.